Spatially-Variant Structuring Elements Inspired by the Neurogeometry of the Visual Cortex

Miguel A. Luengo-Oroz

Biomedical Image Technologies, Universidad Politécnica de Madrid, Spain
maluengo@die.upm.es

Abstract. The V1-region of the primary visual cortex performs contour integration in the early mammalian visual system. The geometry of the neural connections of the V1-region has been mathematically described as a roto-translational continuous space. In this work, a bio-inspired methodology for processing 2D images based on the V1-region neurogeometrical structure is proposed. The input image is first transformed into the 3D roto-translational space. Then spatially-variant mathematical morphology operators using helicoidal structuring elements are applied in order to mimic the neural processing in the primary visual cortex. Finally, the output is projected back to the 2D cartesian space. Some illustrative straightforward applications of this methodology are presented for contour-completion and object-occlusion 2D problems.

1 Introduction

One of the most fascinating properties of the mammalian visual system is its capability for binding and segmenting incomplete patterns as illusory contours, i.e. the famous Kanizsa triangle (see Fig. 1). The primary visual cortex is said to play a fundamental role in the binding operation. Thus, replicating this behavior can be extremely useful for image analysis methods [1,2,3]. Other bio-inspired computer vision systems that mimic the first stages of the visual pathways - computer retinas- have been used for edge detection [4] or motion estimation [5]. Concerning the primary visual cortex, previous works of [6,7] have proposed mathematical continuous models for the neural architecture of this region. Computer simulations of neural activity using these models allow to extract illusory contours in the same way that vision does. Furthermore, image processing filtering techniques based on diffusion processes on this neural mathematical space have been proposed [8]. The present article is inspired by the previous mathematical models of the functional architecture of the V1-region in the primary visual cortex. The main idea is to propose a methodology that transforms a 2D image into the 3D roto-translational space and process the data in this 3D space using spatially-variant mathematical morphology. The neural connections are given by helicoidal structuring elements, and neuron synchronization - that produces the contour integration property - is replicated with a morphological filtering. This methodology can be used to effectively approach contour-completion or shape-occlusion image processing problems.

P. Soille, M. Pesaresi, and G.K. Ouzounis (Eds.): ISMM 2011, LNCS 6671, pp. 236–247, 2011.

2 Background

2.1 The Primary Visual Cortex and Its Geometrical Structure

The visual pathway starts in the photoreceptors of the retina, a layer of cells at the back of the eye. The information leaves the eye by way of the optic nerve and arrives at the primary visual cortex, at the back of the brain. The receptive fields of the neurons in the early visual cortex (V1) characterize the response to different light patterns coming from the visual field. This response is frequently selective to oriented stimulus in a small region [9]. Horizontal connections between cells that join regions corresponding to receptive fields not overlapped in the visual field, are in charge of facilitating the contour integration. An important characteristic of the cortical design of V1 is the arrangement of its composing cells (neurons) into orientation columns. One orientation column corresponds to one point in the visual field and the coordinate along the column corresponds to the orientation angle (see Fig. 2). The role of this arrangement is to facilitate communication between cells that have similar orientation preferences but that are located in different visual field positions. There are several anatomical and neurophysiological studies in cats, monkeys, etc. that show the long range connections between cells of similar orientation preference. Furthermore, in [10], it has been shown that these connections extend for a longer distance along the "good continuation" and less in the orthogonal direction. This idea of perceptual binding has been previously described by the Gestalt's psychologists in the 50's [11] and has been formalized as the associative field [12](see Fig. 1), suggesting that a discontinued visual line will tend to be perceptually grouped together if the different segments are aligned or follow a smooth curve. In [6], a geometrical model of the column arrangement is proposed. The orientation columns are considered as vertical fibres distributed over a retinotopic array. Each point of the retinal field $r = (x, y) \in \Re^2$ is associated with the fibration $s = \frac{dx}{dy} \in S^1$. Thus, the geometrical space associated with the cell column arrangement is $(\Re^2, S^1)$, the roto-translational group [7]. In this organization, the arrangement of neighbouring fibers ensures all orientations in nearby columns are in a position to interact between them. When a signal arrives at the retinotopic field, it passes to the visual cortex and the signal is converted into the V1-column model: $\Re^2 \rightarrow (\Re^2, S^1)$. Afterwards, each cell acts as a single processor that interacts with its cell neighborhood regarding its geometrical context.

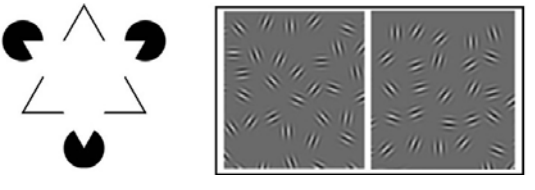

Fig. 1. (left) Kanizsa's triangle. (right) Although both images have similar statistic properties, we "see" a continuous line on the left image.

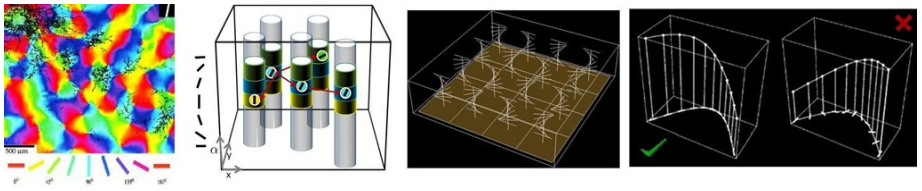

Fig. 2. From left to right. (1)Relationship between orientation columns and long range horizontal connections revealed in optical imaging of tree shrew V1 region combined with injection of biocytin tracer. Different colors represent the different orientation columns. The white dots represent the region where an anatomical tracer is injected. The black dots represent axonal terminals colored by this process. Long range interactions tend to concentrate in cortical regions that share similar orientation specificity with the injection site. Shorter range interactions span other orientations, the more orthogonal with the initial orientation, the shorter the interaction [extracted from [10]]. (2) Schematic representation of column organization with longer horizontal inter-columnar connections between iso-orientation cells. (3) Arrangement of preferred orientations for columns in the $(\Re^2, S^1)$ space. Cells in a plane with $s = K$ have the same preferred orientation. (4) Not all the arbitrary paths in the 3D volume of $(\Re^2, S^1)$ correspond to a continuous line in the retinotopic field $(\Re^2)$ [adapted from [6]].

When neurons process signals in such a space, contour integration based on the concept of associative field emerges in a simple natural way.

2.2 Mathematical Morphology Basics

In the framework of digital grids, a *binary image* can be represented by a function $f : D_f \to T$, where D_f is a subset of $\mathbf{Z}^2$ and $T = \{0, 1\}$ is an ordered set. Let B be a subset of $\mathbf{Z}^2$ and $\lambda \in \mathbf{N}$ a scaling factor. λB is called *structuring element* (shape probe) B of size λ. The basic morphological operators are dilation $(\delta_B(f(x)) = \sup_{y \in B}\{f(x - y)\})$ and erosion $(\varepsilon_B(f(x)) = \inf_{-y \in B}\{f(x - y)\})$. A dilation by a structuring element λB can by obtained by iteration of the unit structuring element B, hence $\delta_{\lambda B}(f) = \delta_{(\lambda-1)B}\delta_B(f)$ The two elementary operations of *erosion* and *dilation* composed together give opening $(\gamma_{\lambda B}(f) = \delta_{\lambda B}[\varepsilon_{\lambda B}(f)])$ and closing $(\varphi_{\lambda B}(f) = \varepsilon_{\lambda B}[\delta_{\lambda B}(f)])$, that filter out light and dark structures from the images according to a predefined size λ and shape criterion B. Although image processing applications using morphological operators commonly use euclidean-based structuring elements (disk or sphere), recent works propose using different structuring elements in the same image, depending on its contextual or geometric information [13,14,15,16]. In [17], we find a very interesting work that deals with adaptive morphology for edge linking. Generally speaking, the structuring element fixes the metric in the image space.

3 Mimicking Neural Processing with Morphological Operators in the Neurogeometrical Space

0The processing chain of our model works as follows (see Fig. 3): first the input image is lifted into the roto-translational space. Then morphologicaloperators

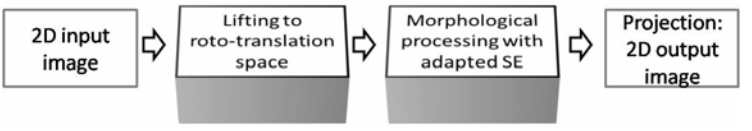

Fig. 3. Processing workflow

mimicking the neural cell-to-cell interactions are performed according to position-dependant structuring elements. The structuring elements are embedded in the $(\mathbb{Z}^2, S^1)$ space. Finally the image is projected back to the image space. This processing can be seen as a filtering process and its properties depend on the morphological operators performed in the roto-translational space.

3.1 Lifting Up Images: From $(\mathbb{Z}^2)$ to $(\mathbb{Z}^2, S^1)$

In the visual system, the signal acquired by photoreceptors in the retina is transformed into an active pattern in the neural hypercolumn structure of the visual cortex. Similarly, in our system, the signal passes from the image space $f \in (\mathbb{Z}^2)$ to the roto-translational space $f' \in (\mathbb{Z}^2, S^1)$. This procedure can easily be done by means of morphological linear openings: $f'(x, y, s) = \gamma_{B(s)}(f(x, y))$, where $B(s)$ corresponds to a line structuring element with a rotation angle of s (see Fig. 4). Note that the process of lifting is inherently imperfect (due to the discretization of the angle) and its precision should be carefully evaluated in future research [18]. For simplicity, in the examples showed in this article, a nearest neighbor approximation has been used to calculate the segments rotated at different angles.

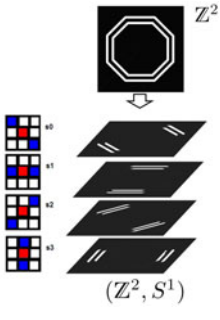

Fig. 4. A simple discrete configuration of $(\mathbb{Z}^2, S^1)$ is illustrated. The S^1 space is decomposed into 4 possible orientations, $\{s0, s1, s2, s3\}$, associated respectively to a rotation angle of $\{-45, 0, 45, 90\}$ degrees. Lifted image is $f'(x, y, s) = \gamma_{B(s)}(f(x, y))$, $s = \{s0, s1, s2, s3\}$. On the left, the structuring elements $B(s)$ associated to each level of S^1.

3.2 Structuring Elements in $(\mathbb{Z}^2, S^1)$

The structuring element (SE) associated with a position in the visual field $r = (x, y)$ and an orientation s models the connections of the neuron at position $p = (r, s) \in (\mathbb{Z}^2, S^1)$. These connections represent the possibilities allowed for

a "good continuation" from p (see Fig. 1). Thus, in each level corresponding to an angle s, there exists a privileged direction associated with the horizontal connections (see Fig. 2). Two points $a(r, s)$ and $b(r', s)$ can be connected if r and r' are in the same straight line of orientation s. Two points $a(r, s)$ and $b(r', s + \Delta s)$, that are not collinear, can be connected if the admitted "good continuation" allows a turn of at least Δs. Consequently, the SE associated with the position p is a partial helicoid whose rotation axis is perpendicular to the plane $\mathbb{Z}^2$. The helicoid rotation angle and its radius are fixed by the turn admitted in the associative field. Globally, the connectivity of the $(\mathbb{Z}^2, S^1)$ space (equivalent to the neural wiring) is given by an SE which is position-invariant for the SE's defined over a plane $s = K$. Let $St_{(r,s)}$ be the SE in the position $p(r, s)$; so $\forall r' \in \mathbb{Z}^2, St_{(r',s)} = St_{(r,s)}$. The SE associated with an orientation s is denoted St_s. As a result of the arrangement of orientation columns, $St_{s+\Delta s} = St_s$ *rotated* Δs. Therefore the SE is position-dependent and it turns when changing the s coordinate (see Fig. 5). Note also that the support of the $(\mathbb{Z}^2, S^1)$ space is periodic along the s coordinate (the planes $s = min$ and $s = max$ are neighbors). All of the paths in the $(\mathbb{Z}^2, S^1)$ space produced by the lift of a 2D image whose content is a continuous connected component, only correspond to a subset of all the possible connected paths with euclidian metric in the 3D space of $(\mathbb{Z}^2, S^1)$. Minimal paths, calculated on the distance function obtained with the metric fixed by the proposed SE's, are equivalent to geodesics in the $(\Re^2, S^1)$ space.

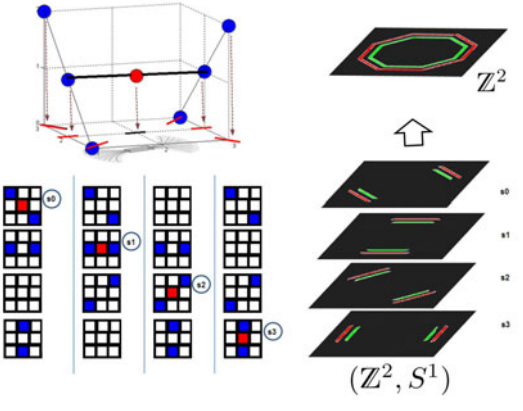

Fig. 5. (top-left) Example of structuring element associated to the space $(\mathbb{Z}^2, S^1)$,$S^1 = \{s0, s1, s2, s3\}$ and its projection on the associative field. The "good continuation" admits a turn of 45 degrees. (bottom-left) The specific SE's in function of the plane $\{s0, s1, s2, s3\}$ where they are located; in red the central point and in blue its neighbors. (right) Labeling of connected elements using the proposed SE's on the lifted image displayed in the previous figure. Results are projected back to $\mathbb{Z}^2$.

3.3 Morphological Neural Processing

The visual cortex is represented by the lattice points and its functionality modeled with a type of simple neural network. Instead of starting from the classical

approach where the state of each neuron is calculated in function of its entries, i.e. $a_i(t+1) = f(\sum_j a_j(t)w_{ji} + \theta_i)$, we chose a dual approach: what is the influence of one neuron on its neighborhood? In the simplest binary mode a neuron propagates an excitatory signal by turning on all the neurons that are connected to it (we denote B_i neurons connected with the axon of neuron i). By analogy, a neuron propagates an inhibitory signal to its neighborhood by turning them off. So the equations that describe the activity $\{0, 1\}$ of a neuron a_i over time are: $a_i(t+1) = \bigvee_{j/i\in B_j} a_j(t)$, and $a_i(t+1) = \bigwedge_{j/i\in B_j} a_j(t)$. The $\bigvee$ (max) equation describes the behavior of an excitatory signal propagation and the $\bigwedge$ (min) equation the inhibitory signal propagation. Each neuron is a pixel and ,in morphological terms, it is connected to its neighbors that correspond to the structuring element associated with that pixel. Excitation and inhibition are also interpreted in terms of morphology as dilation and erosion (see Fig. 6). Therefore the structuring elements define the neural hardware of our system. There is a particularly simple case in these terms,when the cable (ie. a neural fiber) between two cells is bidirectional and therefore cells affected by cell i all affect cell i. These kinds of systems are associated with the symmetric and invariant with respect to translation structuring elements, including segments, squares and hexagons. The simplified equations for a system with these structuring elements are: $a_i(t+1) = \bigvee_{j\in B_i} a_j(t)$, and $a_i(t+1) = \bigwedge_{j\in B_i} a_j(t)$. Therefore, neural wires are completely defined by the structuring elements associated to each position. The evaluation function of each neuron is simplified to a max/min operation, in morphological terms, dilation and erosion (note the iterative and synchronous character of the proposed model is a simplified appoproach, opposed to the asyncronous firing and synchronization of biological neurons in the brain). The mathematical function proposed to perform the contour integration is a closing. A morphological closing is composed by a dilation and its dual erosion ($\varphi_B(f) = \varepsilon_B[\delta_B(f)]$). If the image represents a topographic surface, a morphological closing φ fills channels and lakes and completes partially gulfs. If we interpret the closing sequentially over time in the visual cortex lattice, the dilation models the propagation of an excitatory signal from a single neuron to its neighbors. In case two near neurons are simultaneously activated, a nexus between those two neurons will be created - the perceptive illusion of a line integrated between two points. When an isolated neuron is activated, the sequence of dilations and erosions (=closing) will cause

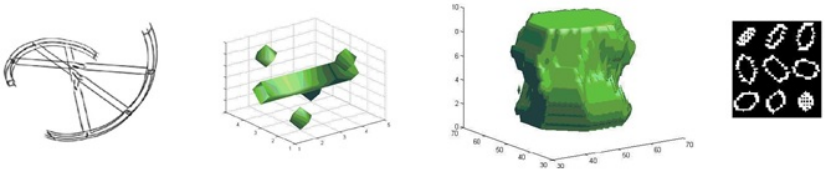

Fig. 6. From left to right: (1) Schematic representation of helicoidal structuring element (similar to DNA double helix organization). (2) Discrete SE with collinear size of 5 pixels. (3) Volume rendering and (4) cross-sections of the wavefront resulting in five iterative dilations of the SE by itself.

the neuron to return to its initial state. The output of the closing operator can be considered as the stable response of the propagation of an excitatory signal (See Fig. 7). Properties of closings can be interpreted as a high level behavior of visual perception. *Increasing*: when vision performs the contour integration, it creates contours but it does not make them disappear. *Idempotent*: regardless of how long we look at an object, this is not going to cause it to change its shape. *Translation invariance*: this property is generally lost in the $(\mathbb{Z}^2, S^1)$ space defined with helicoidal structuring elements, as happens usually in the spatially-variant morphological framework. However, when the translations are made in the $(\mathbb{Z}^2)$ space before lifting up the image to $(\mathbb{Z}^2, S^1)$, the output of the closing operator remains invariant. That means that the translation invariance works only for the subset of translations in $(\mathbb{Z}^2, S^1)$ generated by lifting up objects moved in $(\mathbb{Z}^2)$, corresponding to objects moving in the visual field.

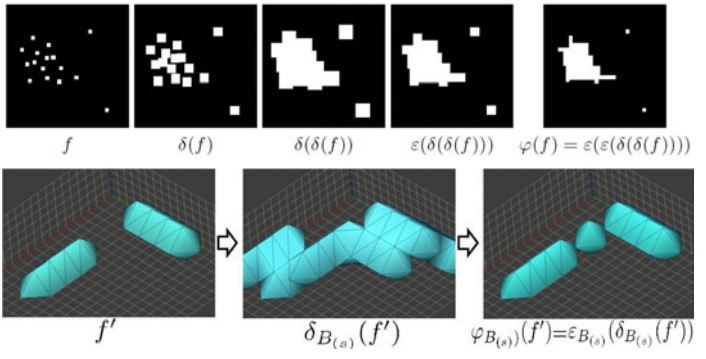

Fig. 7. (top) Illustration of closing properties in a 2D example. Neurons which are next to each other, "synchronize" and fill the gap between themselves according with the utilized structuring element (a square in this example). (bottom) Closing example in $(\mathbb{Z}^2, S^1)$ space, where $S^1 = \{s0, s1, s2, s3\}$ and the structuring elements are those of Fig. 5. A pixel binding the gap between two objects with different orientations is added after closing.

3.4 Projecting Back to the Image Space $(\mathbb{Z}^2)$

In order to come back to the initial image space after performing the morphological closing in the $(\mathbb{Z}^2, S^1)$ space, all the planes at different s levels should be combined, i.e. $f''(x, y) = \bigvee_{\forall s \in S} f'(x, y, s)$. However, for the sake of analysis purposes, we may be interested in maintaining the roto-translation representation. For instance, it would allow us to have two different connected components for two orthogonal crossing lines. In fact, it is this kind of representation that is provided by the V1-region to other brain regions.

4 Application Examples

Hereafter, we present three examples that illustrate the potential applications of transforming and processing 2D images in the roto-translational space. The

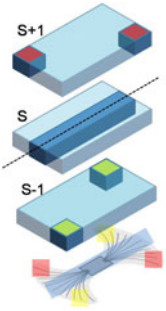

Fig. 8. Example of basic helicoidal SE in a plane S=s. The preferred orientation in this plane is fixed by the dotted axis. The SE is characterized by its size along the preferred (collinear) orientation and the Δs corresponding to the differences of favored orientations between two consecutive planes s and $s+1$. Scaled SE can by obtained by dilating the basic helicoid SE by itself. A projection of the pixels at different orientations belonging to this SE is shown in the lowest plane.

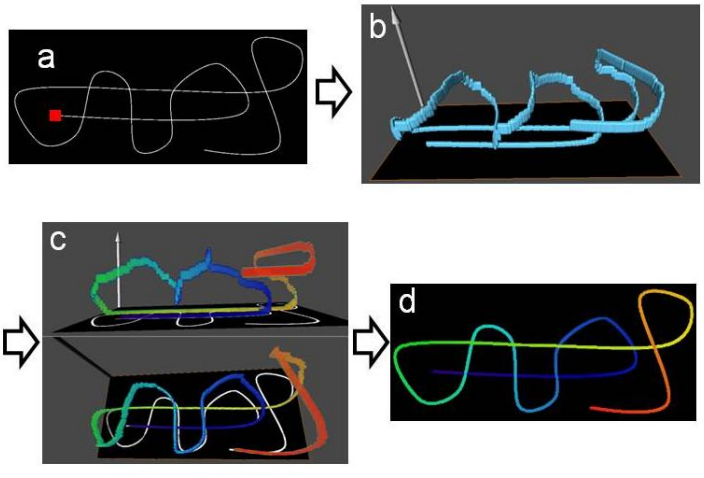

Fig. 9. Distance calculation on tangled line. *(a)* Input image; the red box is the beginning of the line. *(b)* Input image lifted into the roto-translation space. Image size is $(348, 771, 90)$, the size of the line structuring element (SE) used to lift the image is 11 pixels and ΔS between the preferred orientations of two planes at s and $s+1$ is $180/90 = 2$ degrees. *(c)* Geodesic distance on (b), starting from the red-box location (two different 3D views with the 2D projection in the lowest plane). Color code goes from dark blue (dist= 0) to red (dist= max). *(d)* Projection of (c) into the 2D image space.

unit helicoid SE used in the experiments is explained in Fig. 8. In the first example (Fig. 9), the geodesic distance function in $(\mathbb{Z}^2, S^1)$ is used to measure the length of a continuous tangled line in 2D. Distance function on the crossroads is correctly computed when the angle formed by the two crossing lines is

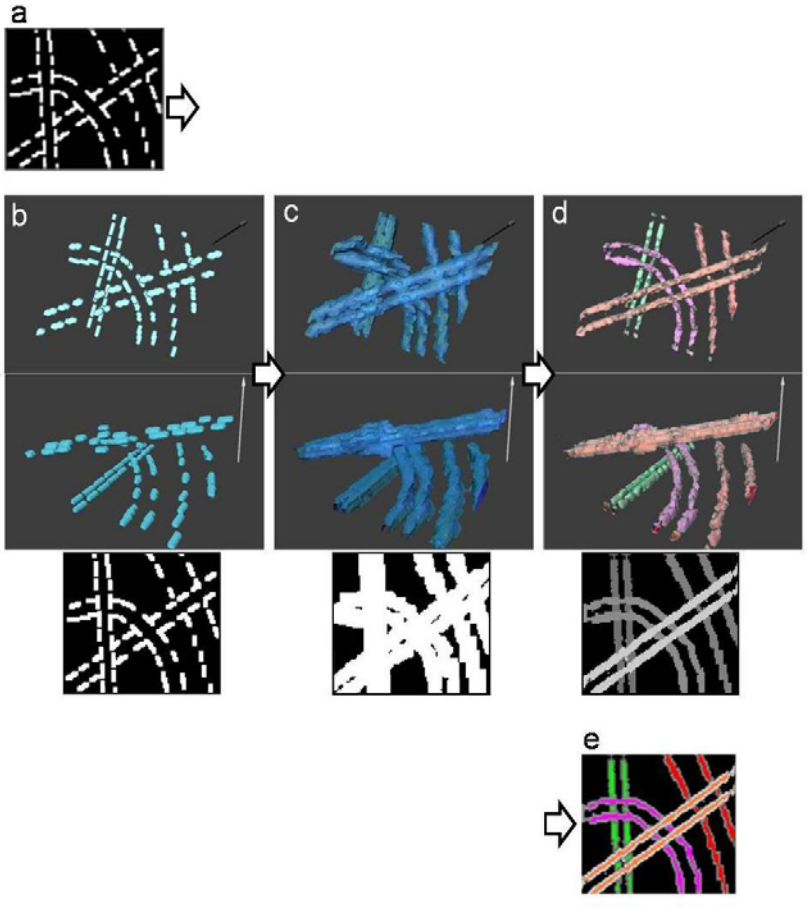

Fig. 10. Perceptual binding of crossing dotted lines. *(a)* Input image. *(b)* Input image lifted into the roto-translation space (volume renderings and projection). Image size is $(98, 100, 45)$, the size of the line SE used to lift the image is 5 pixels and ΔS between the preferred orientations of two planes at s and $s + 1$ is $180/45 = 4$ degrees (2 different 3D views of the image). *(c)* Dilation of (b) by a helicoidal SE formed by the dilation of a basic SE of collinear size of 7 pixels by itself. *(d)* Erosion of (c), therefore $(d) = \varphi(b) = \varepsilon[\delta(b)]$, and labeling of connected components (parallel lines were assigned the same label value). Note that all the original dotted lines are now separated connected components. *(e)* Projection of (d) into the 2D image space (only one color is showed in line crossings).

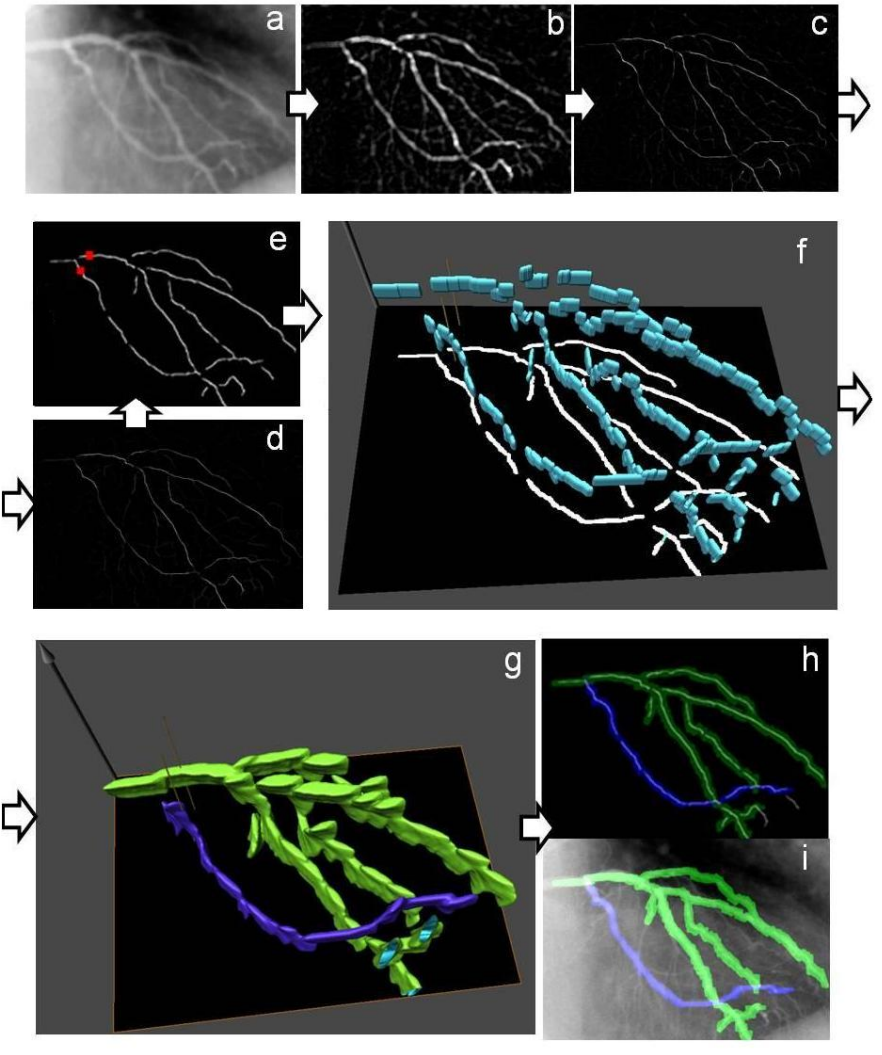

Fig. 11. Main arteries extraction on coronary angiography. *(a)* Input image. *(b)* Top-hat filtering of (a). *(c)* Grey tone homotopic thinning of (b). *(d)* Area opening of (c) . *(e)* Threshold on (d); red-boxes are markers for branch reconstruction. *(f)* Image (e) lifted into the roto-translation space; markers are represented as small thin vertical cilinders. Image size is $(400, 570, 90)$, the size of the line SE used to lift the image is 7 pixels and ΔS between the preferred orientations of two planes at s and $s + 1$ is $180/90 = 2$ degrees. *(g)* Geodesic morphological reconstruction of (f) from markers, (f) has been previously dilated two times by a basic helicoidal SE with a collinear size of 14 pixels. *(h,i)* Reconstructed branches projected to image space and superposed to (e) and (a).

bigger than the turning allowed by the helicoidal structuring element, that is, the connectivity rule in $(\mathbb{Z}^2, S^1)$. The second (Fig. 10) illustrates with a synthetic image how contour integration and disambiguation of occluded objects can be approached by the closing operator in the roto-translation space. Object labeling directly in $(\mathbb{Z}^2, S^1)$ allows to easily separate superposed objects in $(\mathbb{Z}^2)$. The last (Fig. 11) shows a short processing pipeline that identifies the two main vessel trees in a coronary angiography using a reconstruction by dilation operator. Note that, in the presented examples, several SE's corresponding to consecutive orientations are effetively the same due to the discretization of the angle using a nearest neighbour approximation. That means that one pixel at a certain positions migth have been lifted in several consecutive orientation planes of the space $(\mathbb{Z}^2, S^1)$. The question of how to use segments rotated by small angles in a discrete grid is limeted by the segment length and should be deeply explored by means of subpixel accuracy methods.

5 Discussion

We have presented an original bio-inspired image processing methodology that mimics the functions of the early mammalian visual system by transforming a 2D image into a 3D roto-translational space and applying morphological operators in this space. The neural wiring architecture of the V1-area of the visual cortex is replicated by helicoidal spatially-dependent structuring elements and the contour integration property is performed as a morphological filtering. The proposed methodology allows to efficiently approach contour-completion and object-occlusion image processing problems with very reduced mathematical machinery. Several potential applications of this framework can be easily envisaged, i.e. road tracking from satellite imaging or vessel extraction from medical images acquired with projective techniques (i.e. X-ray). The goal of this article is to propose and illustrate the use morphological operators in the roto-translational space. However, future developments should deeply explore the use of more complex morphological operators, different curvature-adapted helicoidal structuring elements and the expansion for grey-level image processing. Overall, this methodology can be used not only for mimicking the binding property of the visual system, but it can also provide a bio-inspired framework for approaching other image analysis problems.

Acknowledgements

This work was partially supported by LA CAIXA grant, FPI and ARTEMIS (Comunidad de Madrid, Spain) and the European Regional Development Funds.

References

1. Kokkinos, I., Deriche, R., Faugeras, O., Maragos, P.: Computational analysis and learning for a biologically motivated model of boundary detection. Neurocomputing 71 (2008)

2. Williams, L.R., Jacobs, D.W.: Stochastic completion fields: A neural model of illusory contour shape and salience. Neural Computation 9(4), 837–858 (1997)
3. Gavet, Y., Pinoli, J.C.: Visual perception based automatic recognition of cell mosaics in human corneal endothelium microscopy images. Image Analysis and Stereology 27, 53–61 (2008)
4. Mertoguno, S., Bourbakis, N.G.: A digital retina-like low-level vision processor. IEEE Transactions on Systems, Man, and Cybernetics, Part B 33(5), 782–788 (2003)
5. Barranco, F., Diaz, J., Ros, E., del Pino, B.: Visual system based on artificial retina for motion detection. IEEE Transactions on Systems, Man, and Cybernetics, Part B 39, 752–762 (2009)
6. Petitot, J., Yannick, T.: Vers une neurogéométrie. Fibrations corticales, structures de contact et contours subjectifs modaux. Mathématiques et sciences humaines 145, 5–101 (1999)
7. Citti, G., Sarti, A.: A cortical based model of perceptual completion in the roto-translation space. Journal of Mathematical Imaging and Vision 24(3), 307 (2006)
8. Sanguinetti, G., Citti, G., Sarti, A.: Image Completion Using a Diffusion Driven Mean Curvature Flowin A Sub-Riemannian Space. In: VISAPP (2), pp. 46–53 (2008)
9. Hubel, D.H., Wiesel, T.N.: Functional architecture of macaque monkey cortex. Proceedings of the Royal Society of London 198, 1–59 (1977)
10. Bosking, W.H., Zhang, Y., Schofield, B., Fitzpatrick, D.: Orientation selectivity and the arrangement of horizontal connections in tree shrew striate cortex. Journal of Neuroscience 17(6), 2112–2127 (1997)
11. Kanizsa, G.: Organization in vision: Essays on gestalt perception (1979)
12. Field, D.J., Hayes, A., Heiss, R.F.: Contour integration by the human visual system: Evidence for a local" association field."., Vision Research 33(2), 173–193 (1993)
13. Debayle, J., Pinoli, J.C.: Spatially adaptive morphological image filtering using intrinsic structuring elements. Image Analysis and Stereology 24, 145–158 (2005)
14. Bouaynaya, N., Charif-Chefchaouni, M., Schonfeld, D.: Theoretical Foundations of Spatially-Variant Mathematical Morphology . IEEE Transactions on Pattern Analysis and Machine Intelligence 30(5), 823–836 (2008)
15. Luengo-Oroz, M.A., Angulo, J.: Cyclic Mathematical Morphology in Polar-Logarithmic Representation. IEEE Transactions on Image Processing 18(5) (2009)
16. Verdú-Monedero, R., Angulo, J.: Spatially-Variant Directional Mathematical Morphology Operators Based on a Diffused Average Squared Gradient Field. In: Proceedings of the 10th ICACIVS, pp. 542–553. Springer, Heidelberg (2008)
17. Shih, F.Y., Cheng, S.: Adaptive mathematical morphology for edge linking. Information Sciences 167(1-4), 9–21 (2004)
18. Hendriks, C., Van Vliet, L.: Using line segments as structuring elements for sampling-invariant measurements. IEEE Transactions on Pattern Analysis and Machine Intelligence, 1826–1831 (2005)